International Journal of Research
Available at https://edupediapublications.org/journals
e-ISSN: 2348-6848
p-ISSN: 2348-795X
Volume 04 Issue 09
August 2017

Fuzzy Based Speed Control of Srm Drive for Pv Integrated Ev System

Shaik Kousar Sana & U.Sravya

M-tech (PE & ED) Student Scholar Department of Electrical & Electronics Engineering, DVR & DR.HS MIC College of Technology, Kanchikacherla; Krishna (Dt); A.P, India.

Assistant Professor Department of Electrical & Electronics Engineering, DVR & DR.HS MIC Collegeof Technology, Kanchikacherla; Krishna (Dt); A.P, India.

Abstract: *This project presents the use of fuzzy logic control (FLC) for switched reluctance motor (SRM) speed. Switched Reluctance Motors (SRM) has a wide range of industrial applications because of their advantages over conventional AC/DC Drives. This is due to simple construction, ruggedness and inexpensive manufacturing potential. Various methods have used and applied to control SRM speed generally, the PV-fed EV has a similar structure to the hybrid electrical vehicle, whose internal combustion engine(ICE) is replaced by the PV panel. The PV has different characteristics to ICEs, the maximum power point tracking (MPPT) and solar energy utilization are the unique factors for the PV-fed EVs.. The main objective of this work is to compare the operation of PI based conventional controller and gives the effective performance using Fuzzy Logic Control. The present work concentrates on the design of a fuzzy logic controller for the SRM speed control. Thus the result of applying fuzzy logic controller to a SRM drive gives the best performance and high robustness than a conventional PI controller. In order to achieve low cost and flexible energy flow modes, a low cost tri-port converter is proposed in this paper to coordinate the PV panel, SRM and battery. The FLC performs a PI-like control strategy, giving the current reference variation based on speed error and its change. And FLC is used for improving the speed response. The performance of the drive system was evaluated through MATLAB/SIMULINK software.*

Key Words: Electric vehicles, photovoltaic (PV), power flow control, switched reluctance motors (SRMs), tri-port converter, Fuzzy Logic Controller.

I. INTRODUCTION

Photovoltaic Generators (PV) provide a clean and unlimited source of energy [1-3]. As part of an ongoing project on low-cost PV powered Electrical Vehicles, a control system is evaluated here for a specific configuration, based on PV panels that power a Switched Reluctance Motor, using independent controllers for maximizing the power supply and optimizing the operation of the motor [4]. In this paper the simulink model for the speed control of switched reluctance motor is carried out by using different speed controllers. The simulink models is designed for P, PI & Fuzzy logic controller separately and their performance result is been compared [5]. The Switched Reluctance Motor is an electric motor which runs by a reluctance torque. For industrial application very high speed of 50,000 rpm motor is used [6-8]. The speed controllers applied here are based on conventional P& PI Controller and the other one is AI based Fuzzy Logic Controller [9].

The PI Controller proportional integral controller) is a most special case of the PID controller in which the derivative of the error is not being used [10]. Fuzzy logic controller is a most intelligent controller which uses a fuzzy logic to process the input. Fuzzy logic is a many valued logic which is much like a human reasoning [11]. In the industrial control FLC has various applications, particularly where this conventional control design techniques are very difficult to apply. A comprehensive review has done for SRM machine modeling, design and simulation and analysis and control.

To provide the maximum possible power in varying conditions, the control system aims to regulate the PV generators so that they are always at the Maximum PowerPoint (MPP) (which changes with the values of solar radiation and panel temperature and with the characteristics of the load connected to the PV) [12]. Therefore, a Maximum Power Point Tracking (MPPT) strategy is used in order to obtain the maximum available power from the panel. Many methods have been developed to determine Maximum Power Point Tracking (MPPT): This paper considers the problem of coupling these energy sources to power an electrical motor in an off-grid application. When a SRM load is supplied from the PV generator via a SEPIC converter then the duty cycle is controlled using a specific MPPT controller. In this study, the converter duty cycle is calculated and adjusted in order to maximize power operation of the whole installation.

The popular electronic method for torque ripple reduction is based on the optimization of control principles. This includes the supply voltage, turn–on and turn–off angles of the converter and current levels [13]. But overall torque will be reduced. Precise control of SRM model is not easy using conventional method (like PI) as its flux linkage, inductance, and torque possess mutual coupling with rotor position and phase current. Fuzzy logic is one of the artificial intelligence techniques, but its applications are more recent than other experts systems. It gives smooth output control even for huge variations in input variables [14]. It provides an opening for control system which is normally considered to be not feasible for automation. It can also be hybrid with other algorithms to solve the complex problems

International Journal of Research
Available at https://edupediapublications.org/journals
e-ISSN: 2348-6848
p-ISSN: 2348-795X
Volume 04 Issue 09
August 2017

[15]. Fuzzy logic has been successfully implemented in modeling, process control and military science. Fuzzy logic controller is the most suitable to design the controller for difficult mathematical model due to nonlinearity and impression.

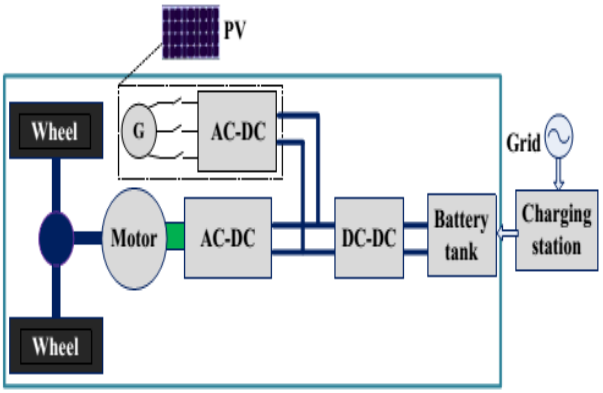

Fig.1 PV-fed hybrid electrical vehicle

II. TOPOLOGY AND OPERATIONAL MODES

A. Proposed topology and working modes

The proposed Tri-port topology has three energy terminals, PV, battery and SRM. They are linked by a power converter which consists of four switching devices (S0~S3), four diodes (D0~D3) and two relays, as shown in Fig.2 [26]. By controlling relays J1 and J2, the six operation modes are supported, as shown in Fig. 3; the corresponding relay actions are illustrated in Table I. In mode 1, PV is the energy source to drive the SRM and to charge the battery. In mode 2, the PV and battery are both the energy sources to drive the SRM. In mode 3, the PV is the source and the battery is idle. In mode 4, the battery is the driving source and the PV is idle. In mode 5, the battery is charged by a single-phase grid while both the PV and SRM are idle. In mode 6, the battery is charged by the PV and the SRM is idle.

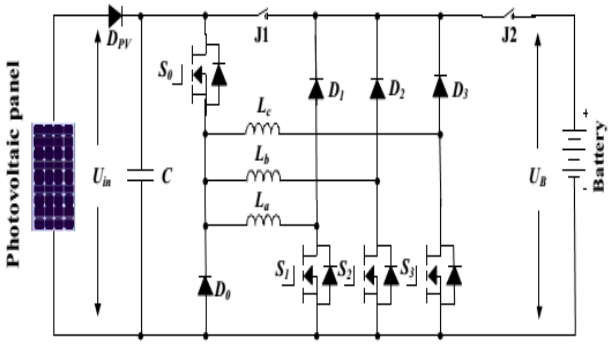

Fig.2. The proposed Tri-port topology for PV-powered SRM drive

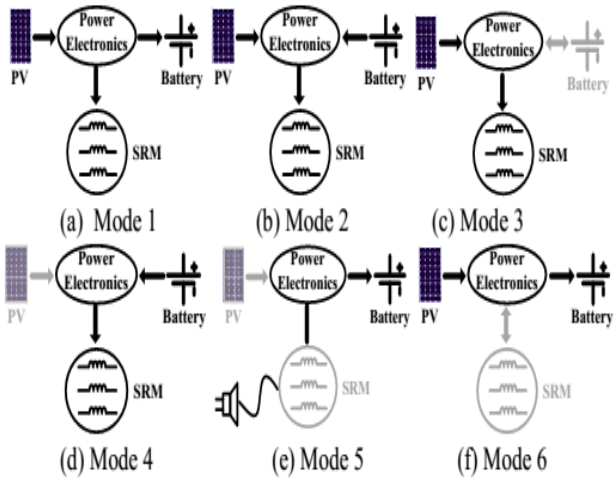

Fig.3. Six operation modes of the proposed Tri-port topology

TABLE 1 J1 and J2 Actions under Different Modes

Mode	J1 and J2
1	J1 turn-off; J2 turn-on
2	J1 and J2 turn-on
3	J1 turn-on; J2 turn-off
4	J1 and J2 turn-on
5	J1 and J2 turn-on
6	J1 turn-off; J2 turn-on

B. Driving modes

Operating modes 1~4 are the driving modes to provide traction drive to the vehicle.

(1) Mode 1

At light loads of operation, the energy generated from the PV is more than the SRM needed; the system operates in mode 1. The corresponding operation circuit is shown in Fig.4 (a), in which relay J1 turns off and relay J2 turns on. The PV panel energy feed the energy to SRM and charge the battery; so in this mode, the battery is charged in EV operation condition.

International Journal of Research
Available at https://edupediapublications.org/journals
e-ISSN: 2348-6848
p-ISSN: 2348-795X
Volume 04 Issue 09
August 2017

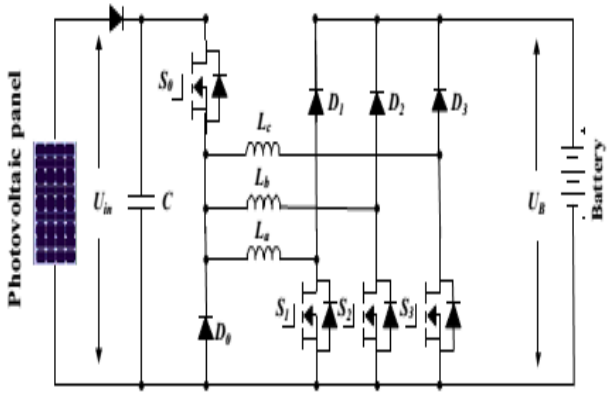

(a) Operation circuit under mode 1

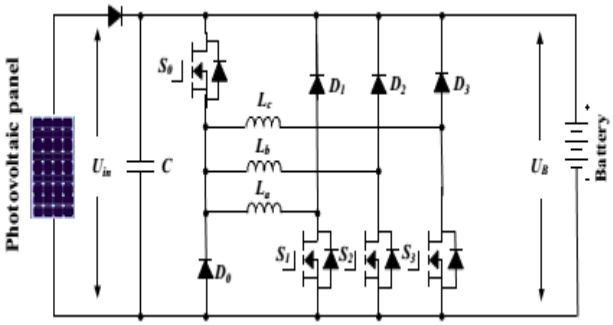

(b) Operation circuit under mode 2

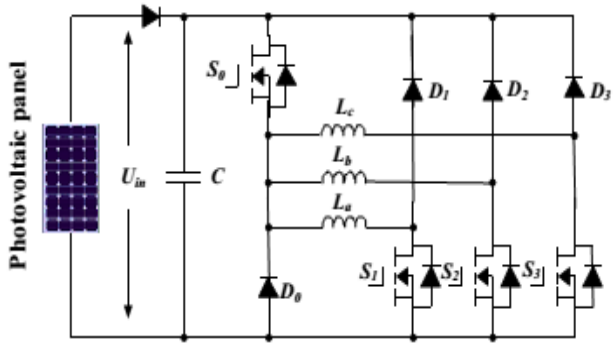

(c) Operation circuit under mode 3

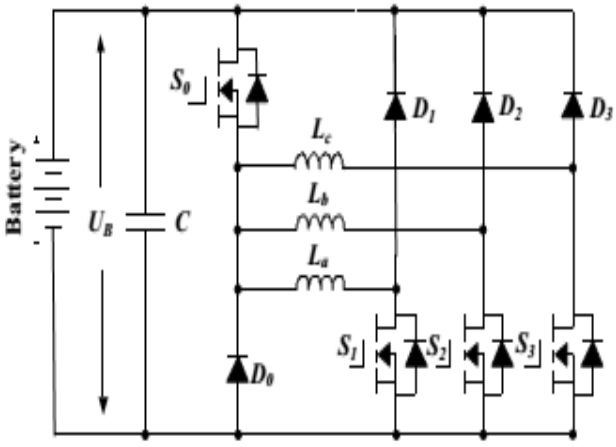

(d) Operation circuit under mode 4

Fig.4 The equivalent circuits under driving modes

(2) Mode 2

When the SRM operates in heavy load such as uphill driving or acceleration, both the PV panel and battery supply power to the SRM. The corresponding operation circuit is shown in Fig.4(b), in which relay J1 and J2 are turned on.

(3) Mode 3

When the battery is out of power, the PV panel is the only energy source to drive the vehicle. The corresponding circuit is shown in Fig.4(c). J1 turns on and J2 turns off.

(4) Mode 4

When the PV cannot generate electricity due to low solar irradiation, the battery supplies power to the SRM. The corresponding topology is illustrated in Fig.4(d). In this mode, relay J1 and J2 are both conducting.

C. Battery charging modes

Operating modes 5 and 6 are the battery charging modes.

(5) Mode 5

When PV cannot generate electricity, an external power source is needed to charge the battery, such as AC grid. The corresponding circuit is shown in Fig.5(a). J1 and J2 turns on. Point A is central tapped of phase windings that can be easily achieved without changing the motor structure. One of the three phase windings is split and its midpoint is pulled out, as shown in Fig.5(a). Phase windings La1 and La2 are employed as input filter inductors. These inductors are part of the drive circuit to form an AC-DC rectifier for grid charging.

(6) Mode 6

When the EV is parked under the sun, the PV can charge the battery. J1 turns off; J2 turns on. The corresponding charging circuit is shown in Fig.5(b).

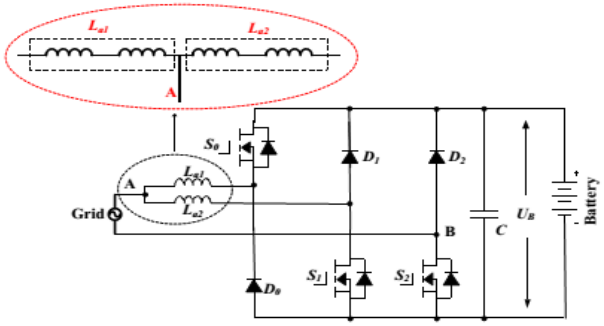

(a) Grid charging mode

International Journal of Research
Available at https://edupediapublications.org/journals
e-ISSN: 2348-6848
p-ISSN: 2348-795X
Volume 04 Issue 09
August 2017

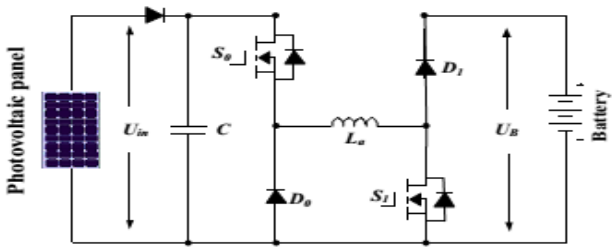

(b) PV source charging mode

Fig.5 Equivalent circuits of charging condition modes

III. Control Strategy under Different Modes

In order to make the best use of solar energy for driving the EV, a control strategy under different modes is designed.

B. Single source driving mode

According to the difference in the power sources, there are PV-driving; battery-driving and PV and battery parallel fed source. In a heavy load condition, the PV power cannot support the EV, mode 2 can be adopted to support enough energy and make full use of solar energy. Fig.6(a) shows the equivalent power source; the corresponding PV panel working points is illustrated in Fig.6(b). Because the PV is paralleled with the battery, the PV panel voltage is clamped to the battery voltage UB. In mode 2, there are three working states: winding excitation, energy recycling and freewheeling states, as shown in Fig.7. Modes 3 and 4 have similar working states to mode 2. The difference is that the PV is the only source in mode 3 while the battery is the only source in mode 4.

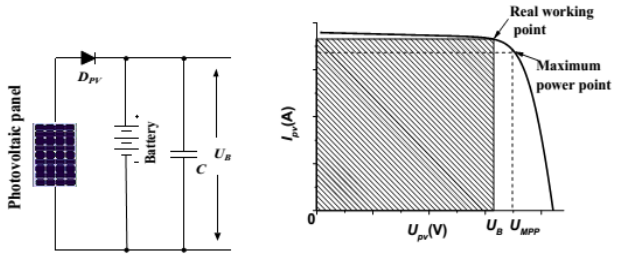

(a) Compound power source (b) Working point of the PV

Fig.6 Power supply at mode 2

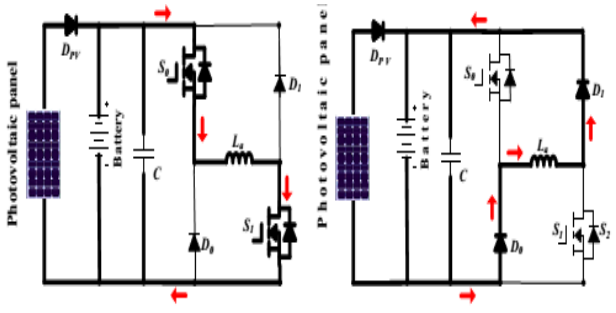

(a) Winding excitation state (b) Energy recycling state

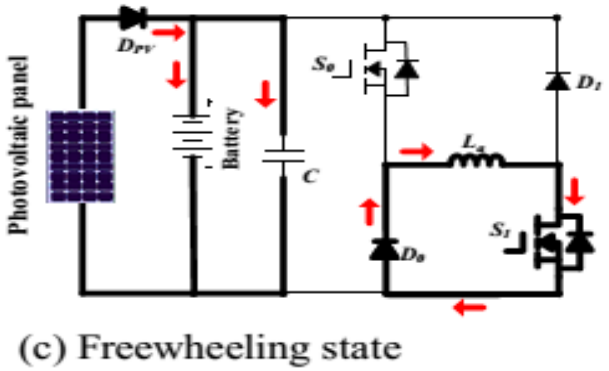

(c) Freewheeling state

Fig.7 Working states at mode 2

Neglecting the voltage drop across the power switches and diodes, the phase voltage is given by

$$U_{\text{in}} = R_k i_k + \frac{d\psi(i_k,\theta_r)}{dt}$$

$$= R_k i_k + L_k \frac{di_k}{dt} + i_k \omega_r \frac{dL_k}{d\theta_r}, \quad k = a,b,c \tag{1}$$

where U_{in} is the DC-link voltage, k is phase a, b, or c, R_k is the phase resistance, i_k is the phase current, L_k is the phase inductance, θr is the rotor position, $\psi(i_k, \theta_r)$ is the phase flux linkage depending on the phase current and rotor position, and ωr is the angular speed. The third term in Eq.1 is the back electromotive force (EMF) voltage given by

$$e_k = i_k \omega_r \frac{dL_k}{d\theta_r} \tag{2}$$

Hence, the phase voltage is found by

$$U_k = R_k i_k + L_k \frac{di_k}{dt} + e_k \tag{3}$$

In the excitation region, turning on S0 and S1 will induce a current in phase a winding, as show in

International Journal of Research
Available at https://edupediapublications.org/journals
e-ISSN: 2348-6848
p-ISSN: 2348-795X
Volume 04 Issue 09
August 2017

Fig.7(a). Phase a winding is subjected to the positive DC bus voltage.

$$+U_{in} = R_k i_k + L_k \frac{di_k}{dt} + e_k \quad (4)$$

When S0 is off and S1 is on, the phase current is in a freewheeling state in a zero voltage loop, as shown in Fig.3.7(c), the phase voltage is zero.

$$0 = R_k i_k + L_k \frac{di_k}{dt} + e_k \quad (5)$$

In the demagnetization region, S0 and S1 are both turned off, and the phase current will flow back to the power supply, as show in Fig.7(b). In this state, the phase winding is subjected to the negative DC bus voltage, and the phase voltage is

$$-U_{in} = R_k i_k + L_k \frac{di_k}{dt} + e_k \quad (6)$$

In single source driving mode, the voltage-PWM control is employed as the basic scheme, as illustrated in Fig.8. According to the given speed ω*, the voltage-PWM control is activated at speed control.

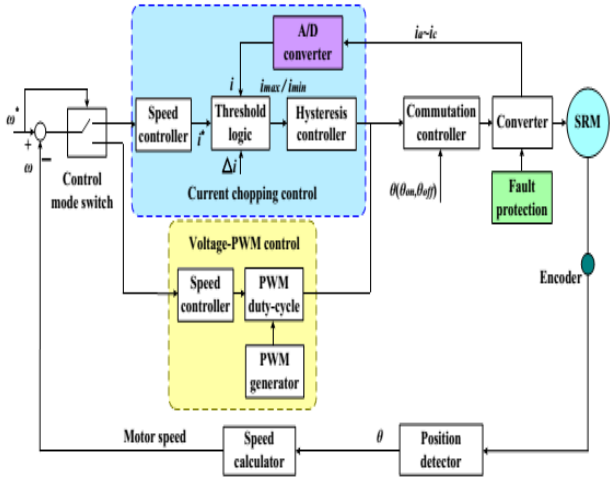

Fig.8 SRM control strategy under single source driving mode

B. Driving-charging hybrid control strategy

In the driving-charging hybrid control, the PV is the driving source and the battery is charged by the freewheeling current, as illustrated in drive mode 1. There are two control objectives: maximum power point tracking (MPPT) of the PV panel and speed control of the SRM.

The dual-source condition is switched from a PV-driving mode. Firstly, the motor speed is controlled at a given speed in mode 3. Then, J2 is tuned on and J1 is off to switch to mode 1. By controlling the turn-off angle, the maximum power of PV panel can be tracked.

There are three steady working states for the dual-source mode (mode 1), as shown in Fig.9. In Fig.9(a), S0 and S1 conduct, the PV panel charges the SRM winding to drive the motor; In Fig.9(b), S0 and S1 turn off; and the battery is charged with freewheeling current of the phase winding. Fig.9(c) shows a freewheeling state.

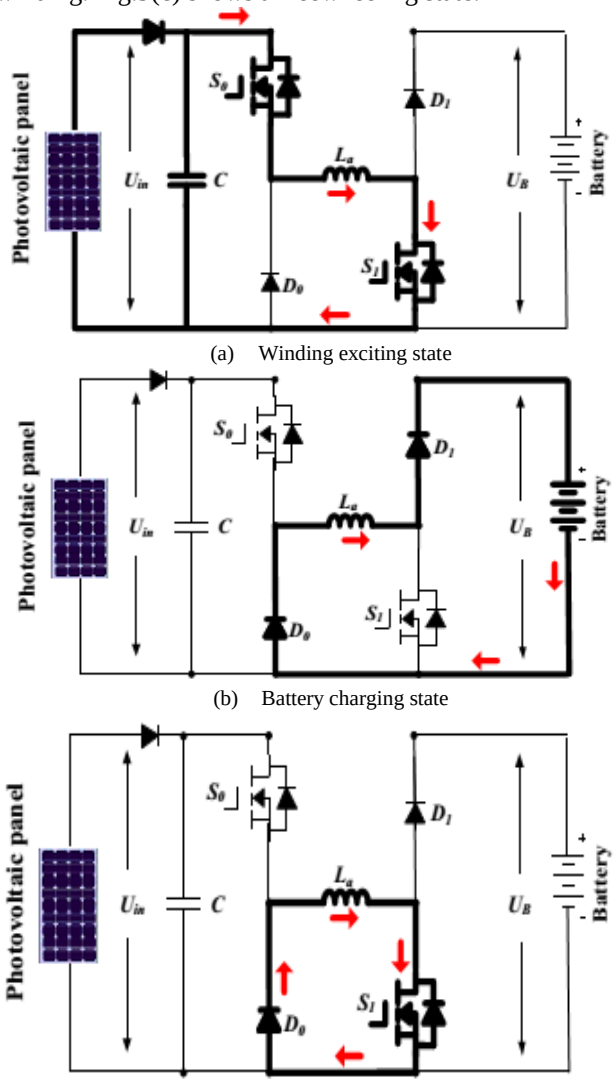

(a) Winding exciting state

(b) Battery charging state

(c) Freewheeling state

Fig.9 Mode 1 working states

Fig.10 is the control strategy under driving-charging mode. In Fig.10, θon is the turn on angle of SRM; θoff is the turn-off angle of SRM. By adjusting turn-on angle, the speed of SRM can be controlled; the maximum power point tracking of PV panel can be achieved by adjusting turn-off angle, which can control the charging current to the battery.

International Journal of Research
Available at https://edupediapublications.org/journals
e-ISSN: 2348-6848
p-ISSN: 2348-795X
Volume 04 Issue 09
August 2017

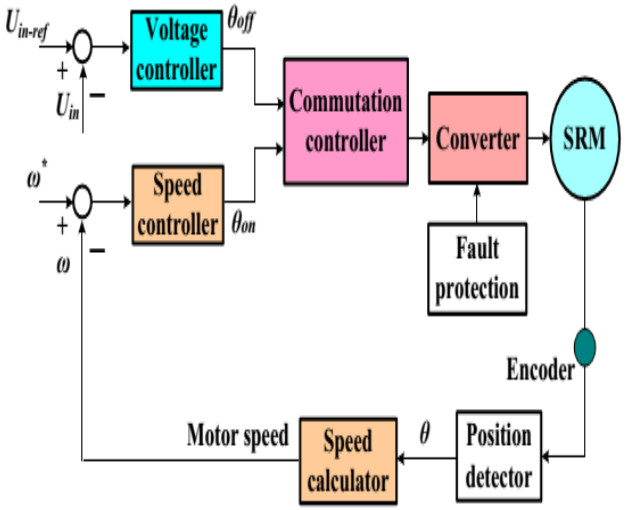

Fig.10. Control strategy under driving-charging mode (mode 1)

C. Grid-charging control strategy

The proposed topology also supports the single-phase grid charging. There are four basic charging states and S0 is always turned off. When the grid instantaneous voltage is over zero, the two working states are presented in Fig.11(a) and (b). In Fig.11(a), S1 and S2 conduct, the grid voltage charges the phase winding La2, the corresponding equation can be expressed as Eq.7; In Fig.11(b), S1 turns off and S2 conducts, the grid is connected in series with phase winding to charges the battery, the corresponding equation can be expressed as Eq.8.

$$U_{grid} = L_{a2} \cdot \frac{di_{grid}}{dt} \tag{7}$$

$$U_B - U_{grid} = L_{a2} \cdot \frac{di_{grid}}{dt} \tag{8}$$

When the grid instantaneous voltage is below zero, the two working states are presented in Fig.11 (c) and (d). In Fig.11(c), S1 and S2 conduct, the grid voltage charges the phase winding La1 and La2, the corresponding equation can be expressed as Eq. (9); In Fig.11(d), S1 keeps conducing and S2 turns off, the grid is connected in series with phase winding La1 and La2 to charges the battery, the corresponding equation can be expressed as Eq.10.

$$U_{grid} = \frac{L_{a1} + L_{a2}}{L_{a1} \cdot L_{a2}} \cdot \frac{di_{grid}}{dt} \tag{9}$$

$$-U_B - U_{grid} = \frac{L_{a1} + L_{a2}}{L_{a1} \cdot L_{a2}} \cdot \frac{di_{grid}}{dt} \tag{10}$$

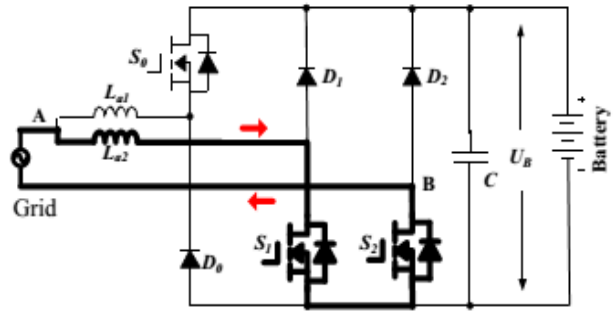

(a) Grid charging state 1 (Ugrid>0)

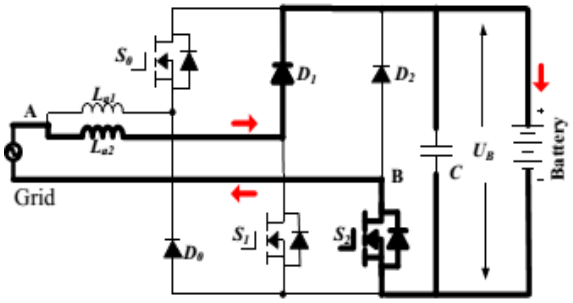

(b) Grid charging state 2 (Ugrid>0)

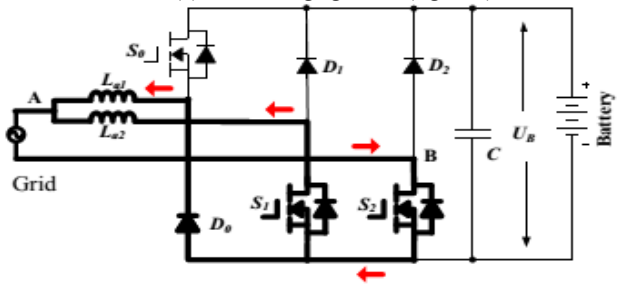

(c) Grid charging state 3 (Ugrid<0)

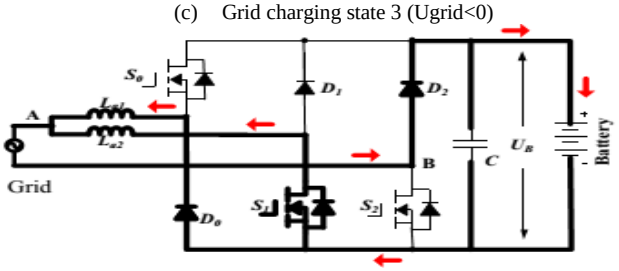

(d) Grid charging state 4 (Ugrid<0)

Fig.3.11 Mode 5 charging states

In Fig.12, Ugrid is the grid voltage; by the phase lock loop (PLL), the phase information can be got; Iref_grid is the given amplitude of the grid current. Combining sinθ and Iref_grid, the instantaneous grid current reference iref_grid can be calculated. In this mode, when Ugrid> 0, the inductance is La2; when Ugrid< 0, the inductance is paralleled La1 and La2; in order to adopt the change in the inductance, hysteresis

International Journal of Research
Available at https://edupediapublications.org/journals
e-ISSN: 2348-6848
p-ISSN: 2348-795X
Volume 04 Issue 09
August 2017

control is employed to realize grid current regulation. Furthermore, hysteresis control has excellent loop performance, global stability and small phase lag that makes grid connected control stable.

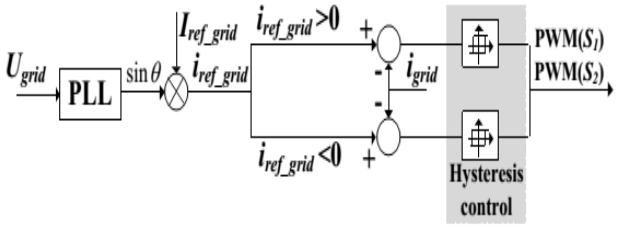

Fig.12 Grid-connected charging control (Mode 5)

D. PV-fed charging control strategy

In this mode, the PV panel charges the battery directly by the driving topology. The phase windings are employed as inductor; and the driving topology can be functioned as interleaved Buck boost charging topology. For one phase, there are two states, as shown in Fig.13(a) and (b). When S0 and S1 turn on, the PV panel charges phase inductance; when S0 and S1 turns off, the phase inductance discharges energy to battery. According to the state-of-charging (SoC), there are three stages to make full use of solar energy and maintain battery healthy condition, as illustrated in Fig.13 (c). During stage 1, the corresponding battery SoC is in 0~SoC1, the battery is in extremely lack energy condition, the MPPT control strategy is employed to make full use of solar energy. During stage 2, the corresponding battery SoC is in SoC1~ SoC2, the constant voltage control is adapted to charging the battery. During stage 3, the corresponding battery SoC is in SoC2~1, the micro current charging is adapted. In order to simplify the control strategy, constant voltage is employed in PV panel MPPT control.

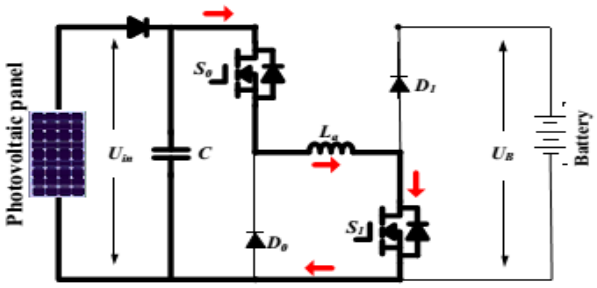

(a) Phase inductance charging

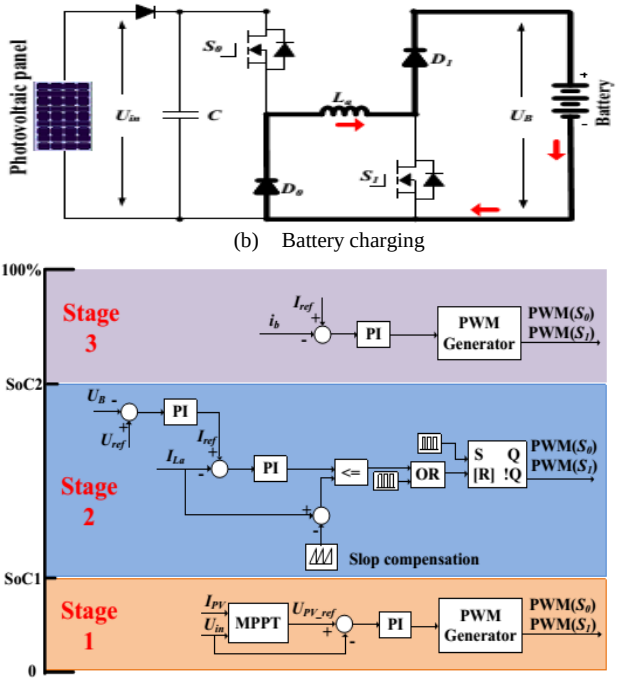

(b) Battery charging

(c) Charging control strategy.

Fig.13 Mode 6 charging states and control strategy.

IV. DESIGN OF A FUZZY CONTROLLER

The Fuzzy control is a methodology to represent and implement a (smart) human's knowledge about how to control a system. A fuzzy controller is shown in Figure.14. The fuzzy controller has several components:

- A rule base that determines on how to perform control
- Fuzzification that transforms the numeric inputs so that the inference mechanisms can understand.
- The inference mechanism uses information about the current inputs and decides the rules that are suitable in the current situation and can form conclusion about system input.
- Defuzzification is opposite of Fuzzification which converts the conclusions reached by inference mechanism into numeric input for the plant.

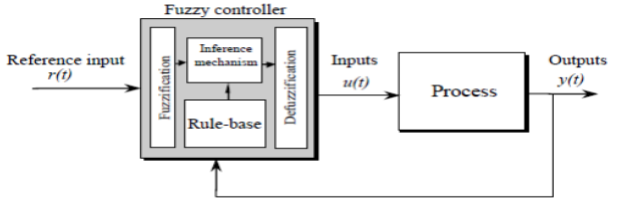

Fig.14 Fuzzy Control System

Fuzzy logic is a form of logic that is the extension of boolean logic, which incorporates partial

International Journal of Research
Available at https://edupediapublications.org/journals
e-ISSN: 2348-6848
p-ISSN: 2348-795X
Volume 04 Issue 09
August 2017

values of truth. Instead of sentences being "completely true" or "completely false," they are assigned a value that represents their degree of truth. In fuzzy systems, values are indicated by a number (called a truth value) in the range from 0 to 1, where 0.0 represents absolute false and 1.0 represents absolute truth. Fuzzification is the generalization of any theory from discrete to continuous. Fuzzy logic is important to artificial intelligence because they allow computers to answer 'to a certain degree' as opposed to in one extreme or the other. In this sense, computers are allowed to think more 'human-like' since almost nothing in our perception is extreme, but is true only to a certain degree.

Table 1: IF-THEN rules for fuzzy inference system

u(t)		e(t)						
		NB	**NM**	**NS**	**ZO**	**PS**	**PM**	**PB**
Δe(t)	**NB**	NB	NB	NB	NB	NM	NS	ZO
	NM	NB	NB	NB	NM	NS	ZO	PS
	NS	NB	NB	NM	NS	NS	PS	PS
	ZO	NB	NM	NS	ZO	ZO	PM	PM
	PS	NM	NS	ZO	PS	PS	PB	PB
	PM	NS	ZO	PS	PM	PM	PB	PB
	PB	ZO	PS	PM	PB	PB	PB	PB

The fuzzy rule base can be read as follows
IF e(t) is NB and Δe(t) is NB **THEN** u(t) is NB
IF e(t) is <negative big> and Δe(t) is <negative big>**THEN** u(t) is <negative big>

V. MATLAB/SIMULATION RESULTS

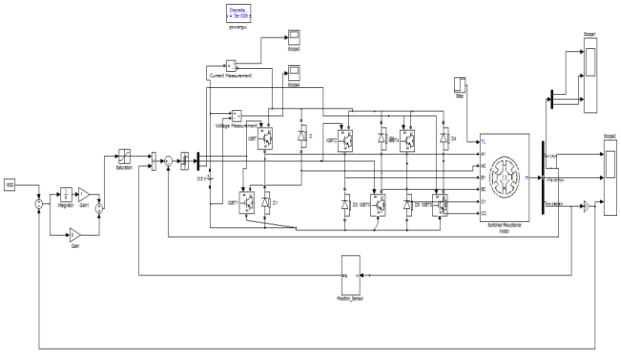

Fig.15 SRM drive model diagram

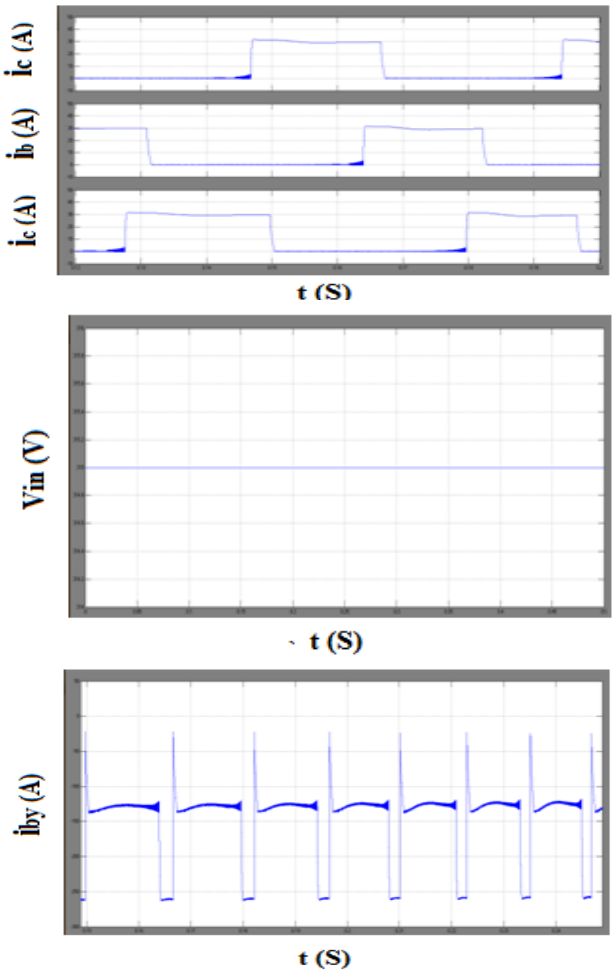

(a) Simulation results of driving-charging mode (mode 1)

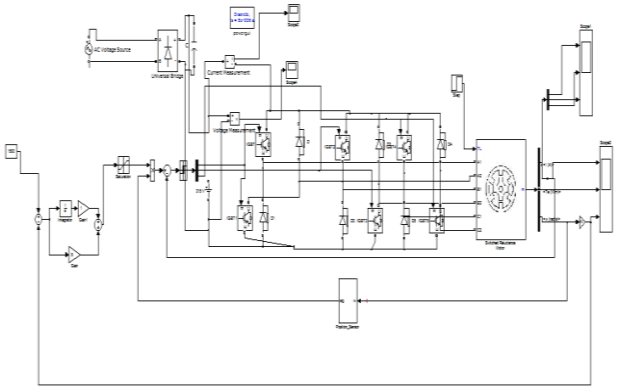

Fig.16 SRM drive model diagram

International Journal of Research
Available at https://edupediapublications.org/journals
e-ISSN: 2348-6848
p-ISSN: 2348-795X
Volume 04 Issue 09
August 2017

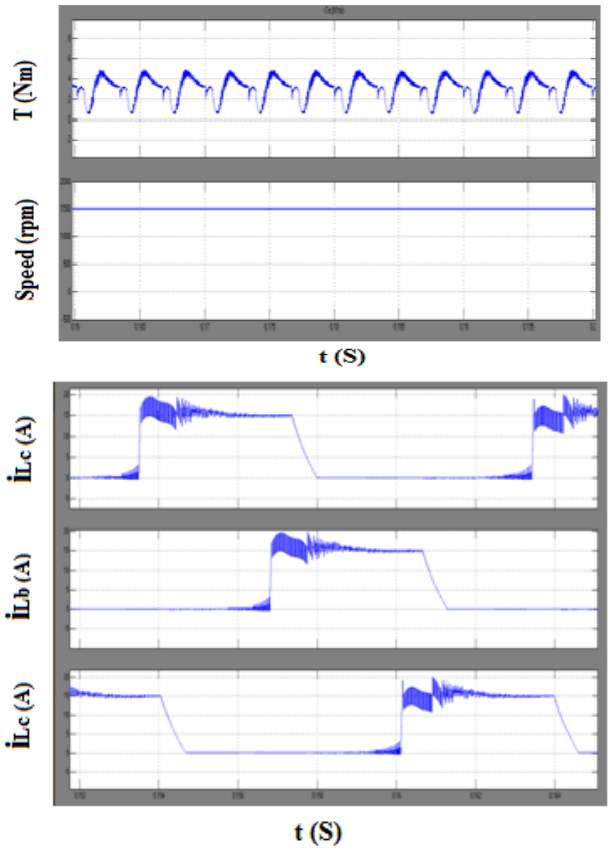

(b) Simulation results of single source driving mode (modes 3 and 4)

Fig.17 Simulation results for driving conditions at modes 1, 3 and 4.

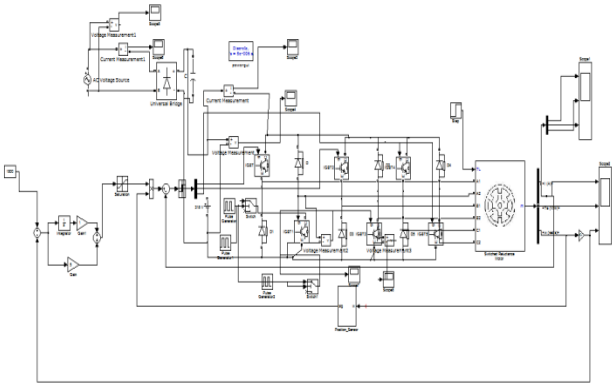

Fig.18 SRM drive model diagram

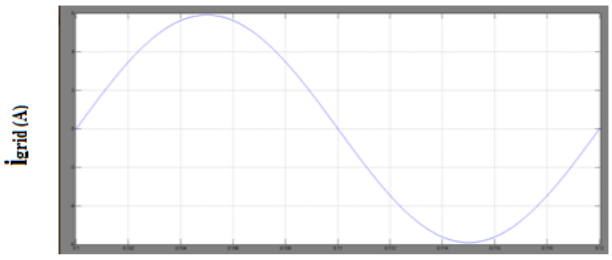

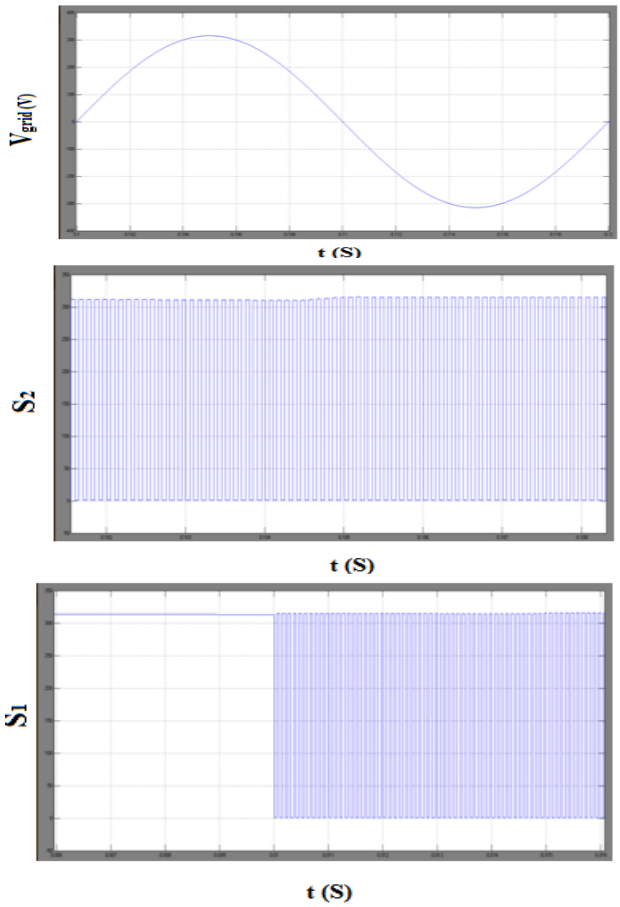

(a) Grid charging (mode 5)

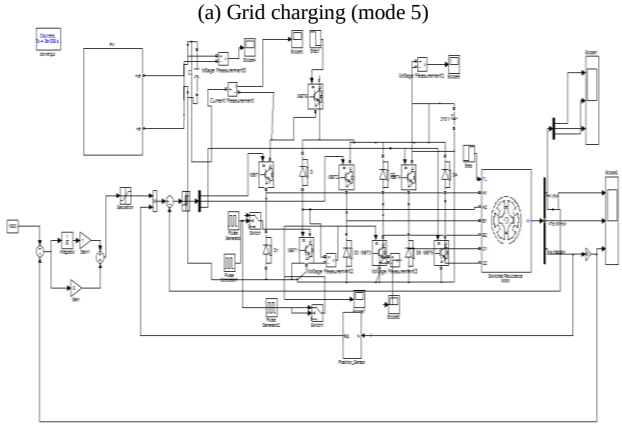

Fig.19 PV-powered SRM drive model diagram

International Journal of Research
Available at https://edupediapublications.org/journals
e-ISSN: 2348-6848
p-ISSN: 2348-795X
Volume 04 Issue 09
August 2017

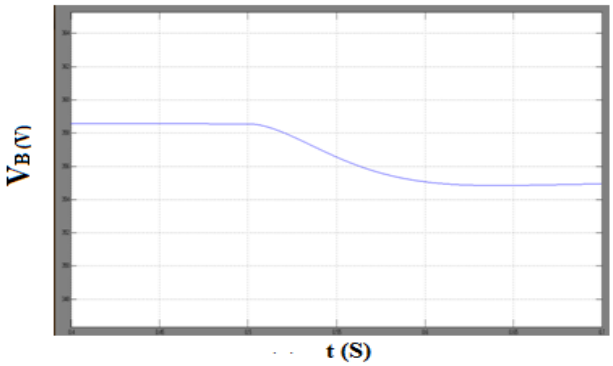

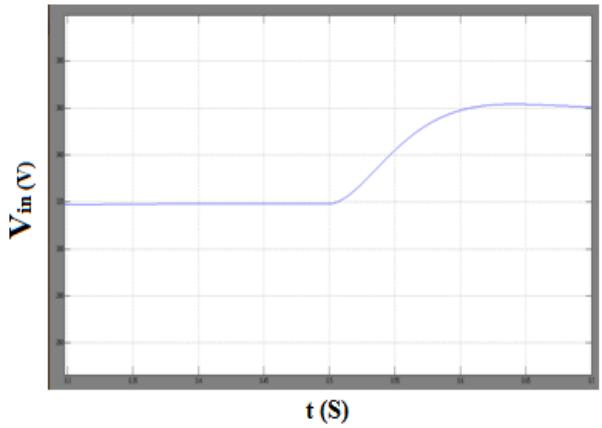

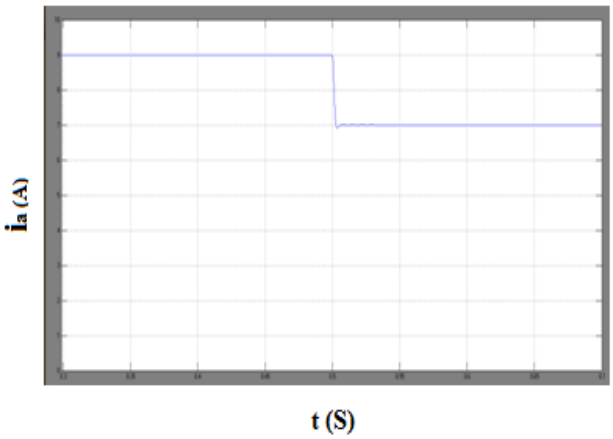

(b) PV charging mode 6 (stage 1 to stage 2)

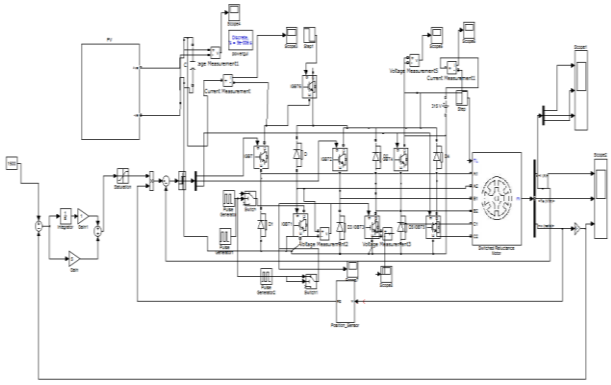

Fig.20 PV-powered SRM drive model diagram

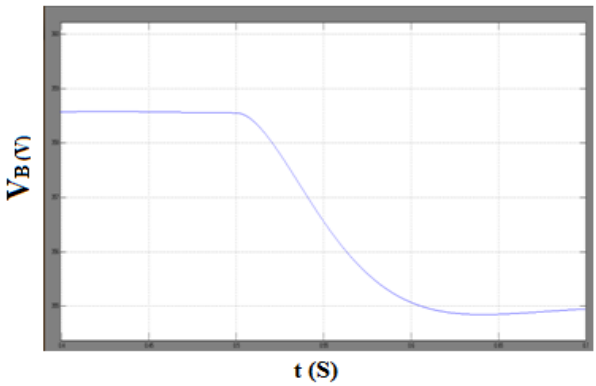

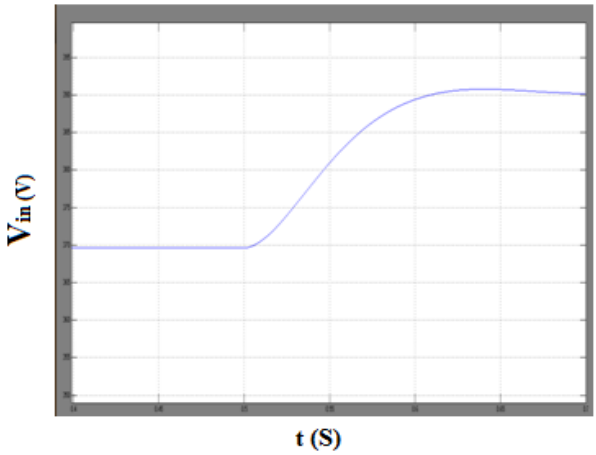

International Journal of Research
Available at https://edupediapublications.org/journals
e-ISSN: 2348-6848
p-ISSN: 2348-795X
Volume 04 Issue 09
August 2017

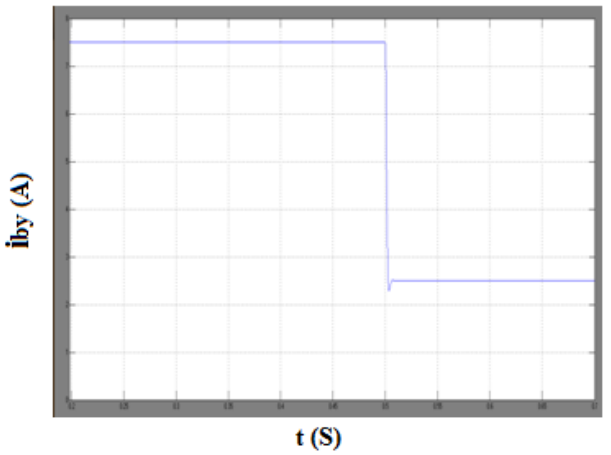

(c) PV charging mode 6 (stage 2 to stage 3)
Fig.21 simulation results for charging modes.

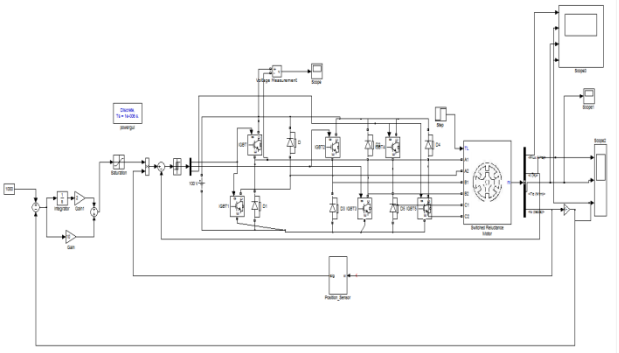

Fig.22 SRM drive model diagram With PI controller

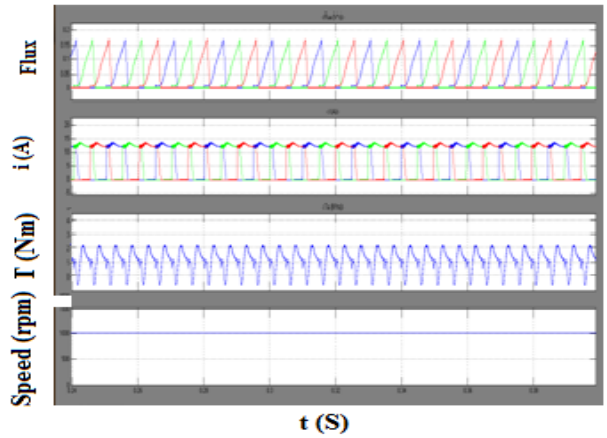

Fig.23 Flux, Current, Speed and Torque

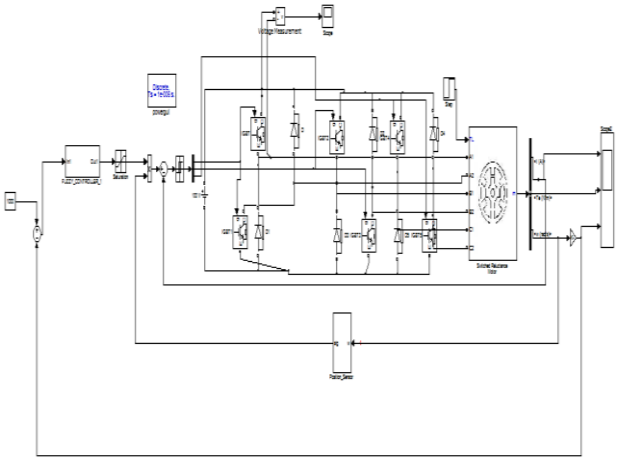

Fig.24 SRM drive model diagram With Fuzzy controller

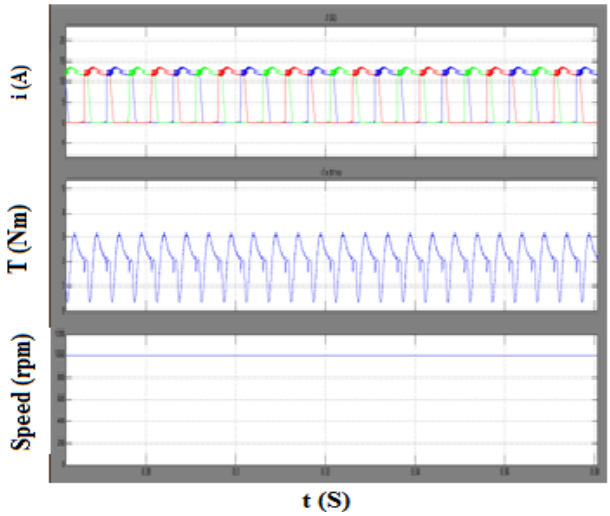

Fig.25 Current, Speed and Torque

VI. CONCLUSION

In order to tackle the range anxiety of using EVs and decrease the system cost, a combination of the PV panel and SRM is proposed as the EV driving system.
The main contributions of this project are:

i. A tri-port converter is used to coordinate the PV panel, battery and SRM.
ii. Six working modes are developed to achieve flexible energy flow for driving control, driving/charging hybrid control and charging control.
iii. A novel grid-charging topology is formed without a need for external power electronics devices.
iv. A PV-fed battery charging control scheme is developed to improve the solar energy utilization.

In conventional methods the speed control of SRM motor is concluded by PI. Here it is executed with Fuzzy Logic Controller. Fuzzy Logic Controller gives the required output than the other controllers. In this proposed method the fuzzy logic controller ensure excellent reference tracking of switched reluctance motor drives. This fuzzy logic controller gives the best speed tracking without overshoot and enhances the speed regulation.

Since PV-fed EVs are a greener and more sustainable technology than conventional ICE vehicles, this work will provide a feasible solution to reducing the total costs and CO_2 emissions of electrified vehicles. Furthermore, the proposedtechnology may also be applied to similar applications such asfuel cell powered EVs. Fuel cells have a much higher powerdensity and are thus better suited for EV applications.

REFERENCES

[1] A. Emadi, L. Young-Joo, K. Rajashekara, "Power electronics and motordrives in electric, hybrid electric, and plug-in hybrid electric vehicles," IEEE Trans. Ind. Electron., vol. 55, no. 6, pp. 2237-2245, Jun. 2008.
[2] Rodrigues MG, Suemitsu WI, Branco P, Dente JA, Rolim LGB. Fuzzy logic control of a switched reluctance motor. Proceedings of the IEEE International Symposium. 1997,2:527–31.
[3] Nagel N. J. and Lorenz R. D., "Modeling of a saturated switched reluctance motor using an operating point analysis and the unsaturated equation", IEEE Trans. Ind. Applicat., Vol. 36, pp. 714-722, May/June 2000.
[4] Z. Amjadi, S. S. Williamson, "Power-electronics-based solutions for plugin hybrid electric vehicle energy storage and management systems," IEEE Trans. Ind. Electron., vol. 57, no. 2, pp. 608-616, Feb. 2010.
[5] A. Kuperman, U. Levy, J. Goren, A. Zafransky, and A. Savernin, "Battery charger for electric vehicle traction battery switch station," IEEE Trans. Ind. Electron., vol. 60, no. 12, pp. 5391-5399, Dec. 2013.
[6] S. G. Li, S. M. Sharkh, F. C. Walsh, and C. N. Zhang, "Energy and battery management of a plug-in series hybrid electric vehicle using fuzzy logic," IEEE Trans. Veh. Technol., vol. 60, no. 8, pp. 3571-3585, Oct. 2011.
[7] C. H. Kim, M. Y. Kim, and G. W. Moon, "A modularized charge equalizer using a battery monitoring IC for series-connected Li-Ion battery Strings in electric vehicles," IEEE Trans. Power Electron., vol. 28, no. 8,pp. 3779-3787, May 2013.
[8] Z. Ping, Z. Jing, L.Ranran, T. Chengde, W. Qian, "Magnetic characteristics investigation of an axial-axial flux compound-structure PMSM used for HEVs," IEEE Trans. Magnetics, vol. 46, no. 6, pp. 2191-2194, Jun. 2010.
[9] A. Kolli, O. Béthoux, A. De Bernardinis, E. Labouré, and G. Coquery, "Space-vector PWM control synthesis for an H-bridge drive in electric vehicles," IEEE Trans. Veh. Technol., vol.62, no.6, pp. 2441-2452, Jul.2013.
[10]http://www. Blue-birdelectric. Net / blue planet _ eco star / solar_assisted_electric_vehicles_sustainable_transport_cars_vans.htm
[11] S. M. Yang, and J. Y. Chen, "Controlled dynamic braking for switched reluctance motor drives with a rectifier front end," IEEE Trans. Ind. Electron., vol. 60, no. 11, pp. 4913- 4919, Nov. 2013.
[12] B. Bilgin, A. Emadi, M. Krishnamurthy, "Comprehensive evaluation ofthe dynamic performance of a 6/10 SRM for traction application in PHEVs," IEEE Trans. Ind. Electron., vol. 60, no. 7, pp. 2564-2575, July.2013.
[13] M. Takeno, A.Chiba, N. Hoshi, S. Ogasawara, M. Takemoto, M. A.Rahman, "Test results and torque improvement of the 50-kW switched reluctance motor designed for hybrid electric vehicles," IEEE Trans. Ind.Appl., vol. 48, no. 4, pp. 1327-1334, Jul/Aug. 2012.
[14] A. Chiba, M. Takeno, N. Hoshi, M. Takemoto, S.Ogasawara, M. A.Rahman, "Consideration of number of series turns in switched-reluctancetraction motor competitive to HEV IPMSM," IEEE Trans. Ind. Appl., vol.48, no. 6, pp. 2333-2340, Nov/Dec. 2012.
[15] I. Boldea, L. N. Tutelea, L. Parsa, and D. Dorrell, "Automotive electric propulsion systems with reduced or no permanent magnets: an overview," IEEE Trans. Ind. Electron., vol. 60, no. 9, pp. 5696- 5710, Oct. 2014.